

# Accretion column eclipses in the X-ray pulsars GX 1+4 and RX J0812.4–3114

D. K. Galloway,<sup>1,2,3</sup> A. B. Giles,<sup>1,4</sup> K. Wu,<sup>2,5</sup> and J. G. Greenhill<sup>1</sup>

<sup>1</sup> School of Mathematics and Physics, University of Tasmania, Hobart 7001, Australia

<sup>2</sup> RCfTA, School of Physics, University of Sydney, NSW 2006, Australia

<sup>3</sup> present address: Center for Space Research, MIT, 37-571 77 Massachusetts Avenue, Cambridge, MA 02139

<sup>4</sup> visitor, USRA/Laboratory for High Energy Astrophysics, Goddard Space Flight Center, Maryland

<sup>5</sup> MSSL, University College London, Holmbury St. Mary, Dorking, Surrey RH5 6NT, UK

31 October 2018

## ABSTRACT

Sharp dips observed in the pulse profiles of three X-ray pulsars (GX 1+4, RX J0812.4–3114 and A 0535+26) have previously been suggested to arise from partial eclipses of the emission region by the accretion column occurring once each rotation period. We present pulse-phase spectroscopy from *Rossi X-ray Timing Explorer* satellite observations of GX 1+4 and RX J0812.4–3114 which for the first time confirms this interpretation. The dip phase corresponds to the closest approach of the column axis to the line of sight, and the additional optical depth for photons escaping from the column in this direction gives rise to both the decrease in flux and increase in the fitted optical depth measured at this phase. Analysis of the arrival time of individual dips in GX 1+4 provides the first measurement of azimuthal wandering of a neutron star accretion column. The column longitude varies stochastically with standard deviation 2–6° depending on the source luminosity. Measurements of the phase width of the dip both from mean pulse profiles and individual eclipses demonstrates that the dip width is proportional to the flux. The variation is consistent with that expected if the azimuthal extent of the accretion column depends only upon the Keplerian velocity at the inner disc radius, which varies as a consequence of the accretion rate  $\dot{M}$ .

**Key words:** accretion — pulsars: individual (GX 1+4) — pulsars: individual (RX J0812.4–3114) — scattering — X-rays: stars

## 1 INTRODUCTION

Binary X-ray pulsars are neutron stars which accrete stellar material from a companion star (e.g. White, Nagase & Parmar 1995). The accretion flow is typically mediated through an accretion disc and accretion columns delineated by the magnetic field of the neutron star ( $B \sim 10^{12}$  G at the surface) which terminate at strongly-emitting regions near the magnetic poles (e.g. Ghosh & Lamb 1979a,b). The plasma flows along the columns from the inner edge of the accretion disc, where the magnetic field begins to dominate the accretion flow, to the magnetic poles (Fig. 1). The base of the columns are expected to cover an arc-shaped region on the neutron star surface as a consequence of the dipolar magnetic field and the limited set of magnetic field lines along which accretion is energetically favourable. To date, observational verification of this scenario has not been possible due to instrumental limitations and a lack of theoretical models describing the anisotropy of X-ray emission from the column. Optical spectroscopic and polarimetric measurements

of accreting white dwarf stars in cataclysmic variables (e.g. Warner 1995) provide corroboration, but such techniques are not available for X-ray pulsars where the accretion columns radiate in X-rays rather than the optical and UV bands. In general there is little observational data available which allow detailed studies of the dynamics of accretion flows.

Sharp (phase width  $\Delta\phi \approx 0.1$ ) dips are usually observed in the pulse profiles of the X-ray pulsars A 0535+26, RX J0812.4–3114 and GX 1+4. These dips have previously been attributed to interactions of the accretion column and the emission region (Čemeljić & Bulik 1998; Reig & Roche 1999; Giles et al. 2000) although supporting arguments have been scarce. A 0535+26 is observed only in outburst, when the X-ray emission is modulated on a period of  $P_{\text{spin}} \approx 103.5$  s (e.g. Negueruela et al. 2000). RX J0812.4–3114, the X-ray counterpart to the B0-1 III-IV star LS 992 was identified from cross-correlation of *ROSAT* galactic plane survey data with SIMBAD OB star catalogues (Motch et al. 1997). Hourly flux variations, as well as X-ray

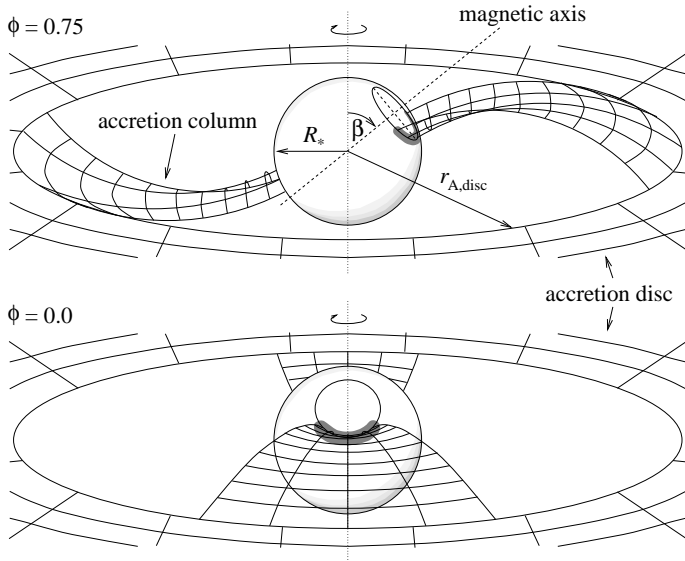


**Figure 1.** Schematic showing the accretion geometry of X-ray pulsars (not to scale). The accreting gas from the companion is thought to form an accretion disc far from the neutron star, which is disrupted at  $r_{A,disc}$  due to the strong (dipolar) magnetic field. Within this radius the accreting matter may only flow along the magnetic field lines, forming two accretion columns terminating at the magnetic poles. Thermal X-ray emission originates from the shaded region at each pole and is Compton scattered by the accretion column plasma above it. Here the magnetic axis is aligned relative to the neutron star rotation axis by  $\beta$  (the magnetic colatitude). The inclination angle  $i$  is such that at phase  $\phi = 0.0$  one of the accretion columns will be closely aligned with the line of sight, giving rise to a partial ‘eclipse’ of the shaded emission region by the accretion column.

pulsations at  $P \approx 31.9$  s were discovered during a *Rossi X-ray Timing Explorer (RXTE)* observation of the source on 1998 February (Reig & Roche 1999). The X-ray behaviour of these Be/X-ray binaries is strongly dependent upon the orbital parameters, and the neutron star spin periods  $P_{spin}$  show a strong correlation with the orbital period  $P_{orb}$  (Corbet 1986). The  $\approx 81$  d periodicity suggested by *RXTE* All-Sky Monitor (ASM) data obtained between 1998–1999 (Corbet & Peele 2000) is consistent with this correlation and probably represents the binary period. The distance was estimated at 9 kpc based on the companion spectral type and interstellar reddening, with a likely uncertainty of 50 per cent (Motch et al. 1997). The pulse profile from the source is strongly asymmetric, with a sharp dip forming the primary minimum. The energy spectrum measured by *RXTE* was fairly typical for X-ray pulsars, and could be adequately fit using a power law model with exponential cutoff (Reig & Roche 1999).

GX 1+4 is the most persistently bright of the three, and possesses the slowest period. Measurements by *RXTE* and the Burst and Transient Source Experiment (BATSE) aboard the *Compton Gamma-Ray Observatory* (Zhang et al. 1995) between 1996–7 found  $P_{spin} = 123.5\text{--}125.5$  s (Galloway & Greenhill 2001, in preparation). The companion to the X-ray source is the 17th magnitude M6 giant V2116 Ophiuchus (Davidsen, Malina & Bowyer 1977), the only known symbiotic binary with a neutron star as the energy

source for the emission line nebula (Belczyński et al. 2000). Regular episodes of relatively rapid spin-up measured from BATSE monitoring of the source suggest an orbital period of  $\approx 304$  d (Pereira, Braga & Jablonski 1999). The distance to the source is thought to be 3–15 kpc (Chakrabarty & Roche 1997). Several estimates of the magnetic field strength are in the range  $2\text{--}3 \times 10^{13}$  G (Beurle et al. 1984; Dotani et al. 1989; Mony et al. 1991; Greenhill et al. 1993; Cui 1997). The dips in this extremely variable source are clearly visible in the X-ray lightcurve when the source is bright and the time resolution is sufficient, and are present in the folded pulse profiles even when the luminosity falls almost to the detection limit (Giles et al. 2000). When the source is bright the dips are broad and generally do not reach zero, while at lower luminosities they are narrower and emission at the dip phase is consistent with the background level. The phase-averaged X-ray spectra from the source are consistent with an approximately thermal spectrum (with temperature  $T_0 \approx 1.3$  keV) modified by Compton scattering within hotter material ( $T_c = 6\text{--}10$  keV) with characteristic optical depth  $\tau = 2\text{--}6$  (Galloway 2000b). The thermal spectrum is thought to arise from the region of the polar cap at the base of the accretion column, with Compton scattering occurring in the hotter plasma above.

## 2 OBSERVATIONS AND ANALYSIS

We undertook a detailed study of the phenomenology of dips in GX 1+4, and to a lesser extent RX J0812.4–3114, using archival *RXTE* satellite observations. Data were obtained using the Proportional Counter Array (PCA; Jahoda et al. 1996), which is sensitive to X-ray photons in the energy band 2–60 keV. Six of the eight event analysers (EAs) aboard *RXTE* are available for processing of events measured by the PCA. Two EAs are dedicated to modes which are always present, ‘Standard-1’ and ‘Standard-2’. The Standard-1 mode features 0.25- $\mu$ s time resolution but only one spectral channel, while Standard-2 offers 128 spectral channels between 0–100 keV (the sensitivity above 60 keV is negligible) accumulated every 16 s. GoodXenon mode data, which offers the maximum 256 channel spectral resolution on 0.9537- $\mu$ s time resolution, was available for most of the observations. Analysis of *RXTE* data presented here was carried out using LHEASOFT 5.0, released 23 February 2000 by the *RXTE* Guest Observer Facility (GOF). Spectral response matrices were calculated for each observation in order to correct for gain changes over the observation period. A separate matrix was calculated for each of the three PCA layers using PCARMF, and then summed using ADDRMF; this was recommended by the PCA team as a workaround to a minor bug in PCARMF which occurs when calculating the response for all layers simultaneously (see [http://heasarc.gsfc.nasa.gov/docs/xte/xhp\\_new.html#bug](http://heasarc.gsfc.nasa.gov/docs/xte/xhp_new.html#bug))

Observations of GX 1+4 were made in 35 separate intervals between 1996 February and 1997 May, with a total exposure time of 230 ks. For a detailed description of the observations and data processing see Galloway (2000b). The pulse period for each observation was determined through folding 1 s lightcurves (with times corrected to the solar-system barycentre) on a range of periods  $P_{trial}$  close to the expected value and calculating the resulting  $\chi^2$ . The most

probable period was found from fitting the peak in the  $\chi^2$  versus  $P_{\text{trial}}$  plot using a gaussian, with errors determined from equivalent analysis on 100 simulated lightcurves. During 1996–1997 GX 1+4 was found to be spinning down at a relatively steady rate, and the pulse period increased from 123.6 s to 125.6 s in the year following 1996 February. The periods measured by *RXTE* are consistent with those from BATSE (Chakrabarty et al. 1997) except when the source was very faint (e.g. 1996 September through November). At these times the the BATSE estimates appear unreliable, exhibiting (apparently) significant variations of  $\pm 0.5$  s on timescales of  $\approx 10$  d. The periods measured by  $P_{\text{trial}}$  folding of *RXTE* data on the other hand increase monotonically throughout this interval.

Two observations of RX J0812.4–3114 were made by *RXTE* on 1998 February 1 and 3 and one on 1999 March 25. The 1999 observation was scheduled at the expected time for an outburst, which have occurred regularly on an  $\approx 81$  d period since 1998 (Corbet & Peele 2000). The measured period for RX J0812.4–3114 was  $P = 31.885623(9) \pm 0.000007(5)$  s, in excellent agreement with the value  $P = 31.8856 \pm 0.0001$  s obtained by Corbet & Peele (2000) for the same observation. Previous spectral analyses for this source used a power-law model with an exponential cutoff (Reig & Roche 1999; Corbet & Peele 2000). Using the recently updated response matrices and faint background models, the cutoff power law model results in generally unacceptable fits, as do power law, power law and blackbody, and broken (two index) power law. Instead the best-fitting spectral model, as for the GX 1+4 observations, was the Comptonisation continuum component of Titarchuk (1994). This analytic approximation is implemented in XSPEC as ‘compTT’ and resulted in a maximum  $\chi^2_{\nu} = 1.5$  for the 1999 March 25 observation. Spectral fit parameters over the three observations were  $T_0 = 1$ –1.2 keV,  $T_e = 5.2$ –6.4 keV and  $\tau = 3.8$ –4.6. In contrast to GX 1+4, no gaussian model component (representing Fe line emission at 6.4–6.7 keV) is required for the spectral fits. The neutral column density  $n_H$  was typically consistent with zero to within the  $1\sigma$  uncertainties. The luminosity in the 2–60 keV energy range reached a maximum during the 1999 March 25 observation of  $(2.57 \pm 0.33) \times 10^{36}$  erg s $^{-1}$  (for a source distance of 9 kpc).

## 2.1 Pulse-phase spectroscopy

The GoodXenon mode data from the 1999 March 25 *RXTE* observation of RX J0812.4–3114 and selected observations of GX 1+4 were divided into 10 equal phase bins, and a spectrum obtained for each phase range. For GX 1+4 the observations on 1996 February 17 and June 8 were chosen for their similar fitted values of  $n_H$  to minimise any potential effects due to variation in this parameter. Additionally, they represent examples of the two apparently distinct groups of GX 1+4 spectra. When  $L_X \gtrsim 2 \times 10^{37}$  erg s $^{-1}$  (2–60 keV, assuming a source distance of 10 kpc),  $\tau = 4$ –6 and  $T_e = 6$ –9 keV typically, while at lower  $L_X$   $\tau \approx 3$  and  $T_e = 7$ –14 keV (Galloway 2000b). The 1996 February 17 observation corresponds to the former case, with  $L_X = (8.5 \pm 3.3) \times 10^{37}$  erg s $^{-1}$ ,  $\tau = 5.6 \pm 0.1$  and  $T_e = 8.1 \pm 0.1$  keV, while on 1996 June 8  $L_X = (1.33 \pm 0.54) \times 10^{37}$  erg s $^{-1}$ ,  $\tau = 2.5^{+0.5}_{-1.1}$  and  $T_e = 13.6^{+5.1}_{-2.6}$  keV ( $1\sigma$  confidence limits). The measured pulse periods during the two observations were 123.6368(1)±

0.0003(8) and 124.1677(0) ± 0.0005(6) s respectively. The ephemeris was chosen so that the primary minimum falls at phase 0.0, with the first bin centred there. Each of the 10 spectra were then fitted with a model identical to that used for the phase averaged spectra, with a Comptonisation component (‘compTT’) and a gaussian component (in the case of GX 1+4) both attenuated by neutral interstellar material.

The greatest spectral variation with phase is typically observed close to the primary minimum (Fig. 2). For the 1996 February 17 observation of GX 1+4, the source spectrum temperature  $T_0$  is generally quite consistent with the phase-averaged value, except at phase  $\phi = 0.0$  where it drops to  $\approx 0.75$  keV. The scattering plasma temperature is also lower at  $\phi = 0.0$  as well as the two adjacent bins, by at most  $\approx 20$  per cent (a  $7.5\sigma$  deviation from the phase-averaged value). The optical depth  $\tau$  exhibits a dramatic increase at the phase of primary minimum, from around 5.6 for the phase-averaged spectrum to more than 10 ( $4.7\sigma$ ). The compTT normalisation (not shown) exhibits the greatest variation of all the parameters, and traces the pulse profile quite well. The  $1\sigma$  confidence limits on the parameters were generally small except at  $\phi = 0.0$ . The spectral variation was symmetric about the primary minimum, as was the pulse profile. The column density  $n_H$  was  $\approx 60\%$  greater than the phase-averaged spectral value around  $\phi = 0.0$  (Fig. 3), but at a significance level of less than  $2\sigma$ . Variation in the Fe line component parameters was no greater than  $1.5\sigma$  with respect to the phase-averaged values over the entire phase range.

The phase variation of spectral fit parameters for the 1996 June 8 observation (not shown) was less significant due to the lower countrate and the wider confidence limits that result. Since the gaussian component parameters were shown to exhibit no significant variation with phase when the source was much brighter, for this analysis they were fixed to values found for the phase-averaged spectrum. Reliable limits on the plasma temperature  $T_e$  could only be determined for phases  $\phi = 0.0$  and 0.1; in the other phase bins the value was instead frozen at the value obtained for the phase-averaged spectrum. The optical depth was greater compared to the phase-averaged level in the phase bins centred on  $\phi = 0.0$  and 0.1. While the maximum enhancement is  $\approx 70\%$  the significance is only  $1.5\sigma$  at best.

Also suffering from a much lower phase-averaged countrate, spectral fitting for the data from RX J0812.4–3114 was substantially more difficult. With all parameters free to vary, the fit values of  $T_0$  and  $n_H$  were poorly constrained, and reliable confidence limits could not be obtained. Following the approach of Galloway et al. (2000), we fixed (‘froze’) these two parameters at the values determined for the phase-averaged spectra, and re-fit the pulse phase spectra. The phase bins centred on  $\phi = 0.0$  and 0.1 again show evidence for reduced  $T_e$  and enhanced  $\tau$  (Fig. 4), although at a significance level of only marginally greater than  $1\sigma$ . While the increase in  $\tau$  coincident with the primary minimum for the latter two observations is not significant, note that the dip is much narrower (particularly for RX J0812.4–3114) than in the 1996 February 17 observation of GX 1+4. Thus the phase bin centered on the primary minimum also covers the dip ingress and egress, and emission during those intervals will tend to dominate the spectrum due to the increased countrate. We suggest that a spectrum taken over

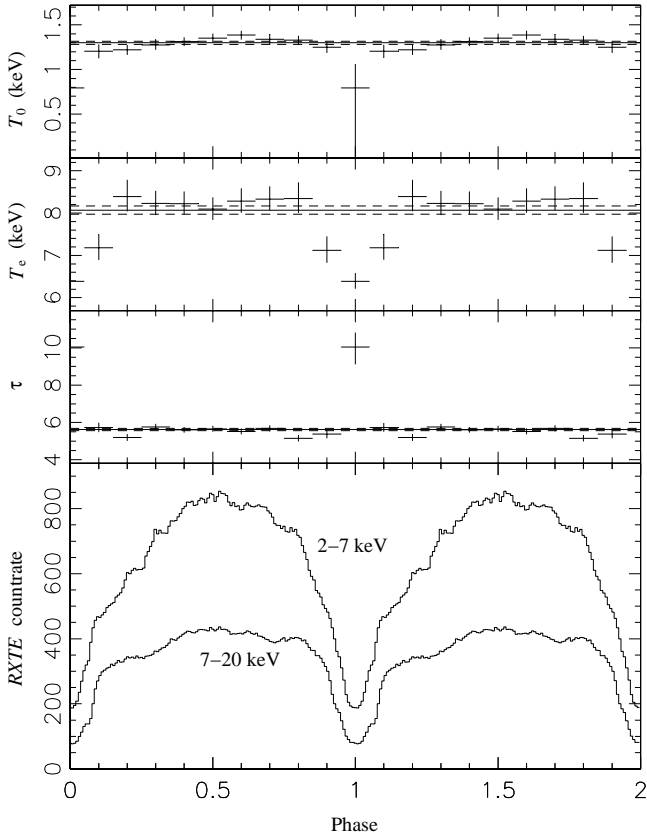


**Figure 2.** Comptonisation component fit parameters versus pulse phase for the 1996 February 17 *RXTE* observation of GX 1+4. The pulse period used is  $P = 123.63681$  s; the ephemeris is defined arbitrarily such that the dip in the pulse profile falls at phase 0.0. From top to bottom, the panels shows the source spectrum temperature  $T_0$ , scattering plasma temperature  $T_e$  and optical depth  $\tau$  and the integrated pulse profile in 2–7 and 7–20 keV energy bands respectively. Fitted parameter values for the phase-averaged spectra covering the same interval are shown by the solid lines; error bars and the dotted lines show the  $1\sigma$  confidence intervals. Two full pulse periods are shown for clarity. The total observing time was 10400 s.

the phases covering only the bottom of the dip may exhibit a much higher  $\tau$ , although *RXTE* does not provide sufficient sensitivity in the present observations to confirm this.

## 2.2 Dip profile measurements in GX 1+4

At moderate countrates the individual dips forming the primary minimum are usually well defined in the 1 s binned lightcurves from GX 1+4. With the exception of the observations with very low countrates (where individual dips could not be unambiguously located), we measured the dip phase variations by calculating the arrival time residuals  $\Delta t_{d,i}$  for the dip from each cycle  $i$ . The expected arrival time is calculated from the mean period for the observation and the ephemeris (used to locate the first observed dip). The actual arrival time is estimated from fitting a parabolic profile to the lightcurve in a 16 s window surrounding the predicted

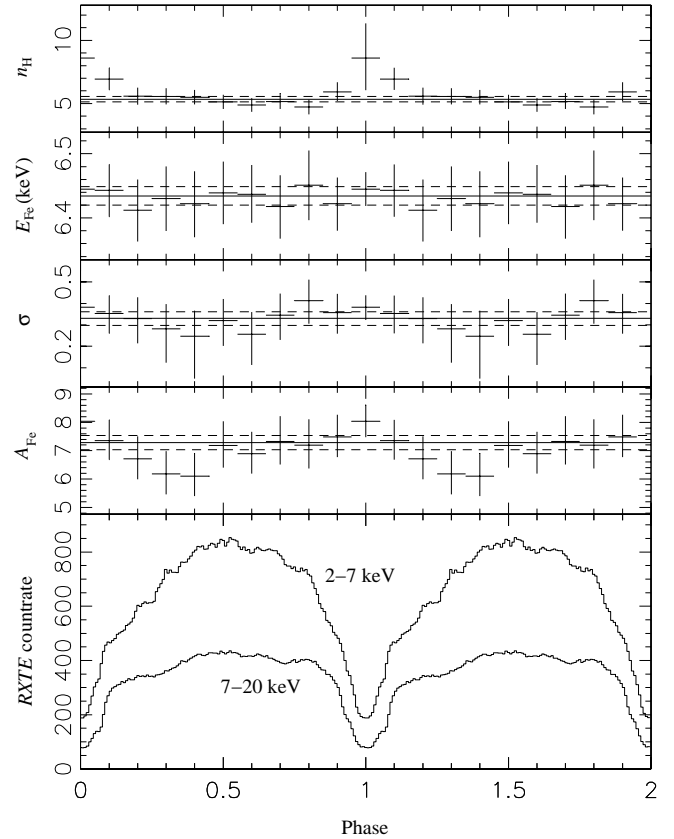


**Figure 3.** Additional spectral model fit parameters versus pulse phase for the 1996 February 17 *RXTE* observation of GX 1+4. From top to bottom, the panels shows the neutral column density  $n_H$  (in units of  $10^{22}$   $\text{cm}^{-2}$ ), Fe line component centre energy  $E_{\text{Fe}}$ , width  $\sigma_{\text{Fe}}$  and normalisation  $A_{\text{Fe}}$  (units of  $10^{-3}$  photons  $\text{cm}^{-2}$   $\text{s}^{-1}$   $\text{keV}^{-1}$ ) and the pulse profiles in the 2–7 and 7–20 keV energy bands. Other details are as for Fig. 2.

arrival time; the arrival time residual is the difference of the two. For the 1996 February 17 observation  $|\Delta t_{d,i}|$  is typically  $\sim 2$  s and may be as much as 4 s (Fig. 5a). Visual inspection of the individual fits confirms that the arrival time errors are genuine and not simply an artefact of poor fits to the dip profiles (for example). The residuals do not appear to exhibit any periodic or quasiperiodic variation with cycle number (time). A search for periodic signals using the Lomb-Scargle periodogram (Press et al. 1996) over all residuals for each of the observations on which the analysis was performed did not result in any significant detections. The most significant peaks were found for low frequency signals in the longest observations, but these detections are most likely aliasing related to observation interruptions due to earth occultations once every 90 min satellite orbit. The standard deviation of the dip residuals  $\sigma(\Delta t_{d,i})$  was found to vary significantly with the mean flux. Above  $L_X \approx 4 \times 10^{37}$   $\text{erg s}^{-1}$  (2–60 keV, assuming a source distance of 10 kpc)  $\sigma(\Delta t_{d,i})$  varies between 1.4–1.9 s, whereas below that level is  $\lesssim 1.3$  s and may be as low as 0.7 s.

The dip phase width  $w_d$  was measured from the mean pulse profiles at a countrate level midway between the mini-

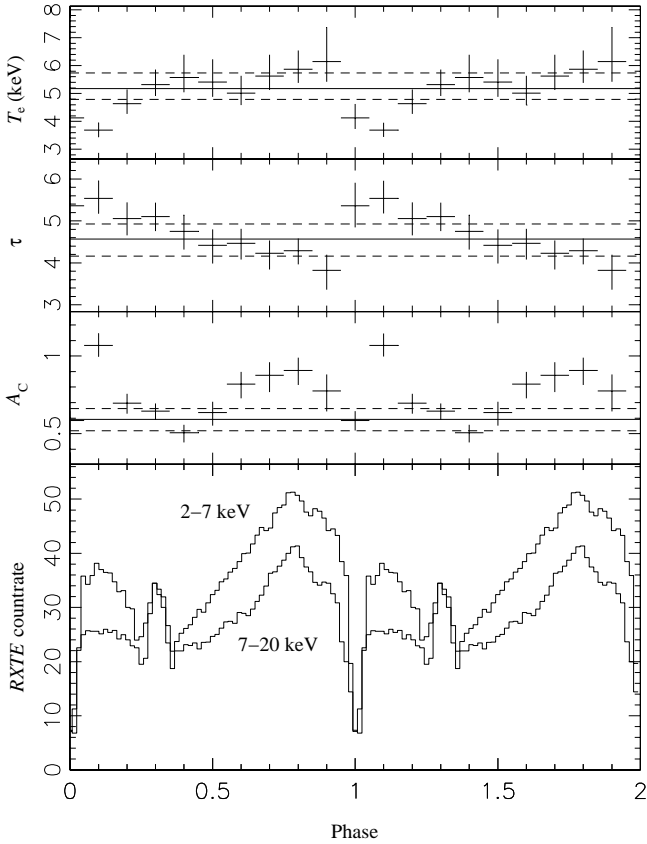


**Figure 4.** Spectral model fitting parameters versus pulse phase for the 1999 March 25 *RXTE* observation of RX J0812.4–3114. Phase selection was undertaken using a period  $P = 31.8856239$  s, with ephemeris chosen arbitrarily so that the primary minimum falls at  $\phi = 0.0$ . From top to bottom, the panels show the scattering plasma temperature  $T_e$ , optical depth for scattering  $\tau$ , normalisation  $A_C$  (in units of  $10^{-2}$  photons  $\text{cm}^{-2} \text{s}^{-1} \text{keV}^{-1}$ ) and the pulse profile in 2–7 and 7–20 keV energy bands respectively. Fitted parameter values for the phase-averaged spectra covering the same interval are shown by the solid lines; error bars and the dotted lines show the  $1\sigma$  confidence intervals. Two full pulse periods are shown for clarity.

imum and the mean level in the phase range 0.8–0.9 and 0.1–0.2. While  $w_d$  varied significantly with  $L_X$  (Fig. 5b, open circles), the dip phase variation described above must account for some if not all of this dependency. Thus an equivalent measure was made using the width parameter from the parabolic fitting divided by the mean count rate over the fitting window, averaged over each observation. While this measurement could not be made over the entire flux range, the resulting dip width does indeed show less variation with  $L_X$  (Fig. 5b, filled circles) and in particular was substantially lower at the highest luminosity, where the dip arrival time residuals are greatest.

### 3 DISCUSSION

RX J0812.4–3114 provides another example of an X-ray pulsar after GX 1+4 whose mean spectra are broadly consistent

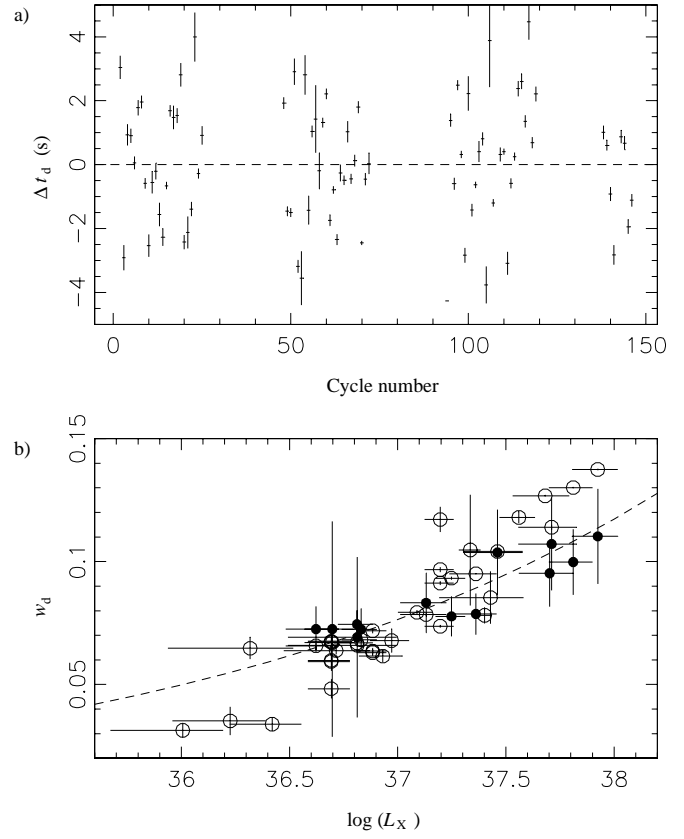


**Figure 5.** Dip analysis results from GX 1+4. a) Typical dip arrival time residuals  $\Delta t_{d,i}$  plotted against cycle number  $i$  for *RXTE* observations of GX 1+4 on 1996 February 17. The  $\Delta t_{d,i}$  from each cycle is the difference between the expected dip arrival time (based on the mean pulse period measured over the entire observation) and the observed time from fitting a parabola to the lightcurve in a 16 s window centred on each dip. Missing cycles are a consequence of occultations of the source by the Earth and passages of the satellite through the South Atlantic Anomaly (SAA). b) Dip width  $w_d$  from 35 separate *RXTE* observations of GX 1+4 between 1996 February and 1997 May and comparison with the theoretical relationship. The dip width calculated from the mean pulse profile is plotted as open circles, while the averaged calculated from individual dip widths is plotted as filled circles. The  $x$ -axis is the log of the 2–60 keV flux in  $\text{erg s}^{-1}$ , assuming a source distance  $d = 10$  kpc. The actual distance is thought to be 3–15 kpc (Chakrabarty & Roche 1997). The dashed line represents the theoretical calculation (equation 2). Error bars represent the  $1\sigma$  uncertainties.

with Comptonisation continuum components. In contrast to GX 1+4, the properties of this source are probably typical of many others, since Be/X-ray binaries make up a significant proportion of all known X-ray pulsars. The phase-averaged spectral fit parameters fall within the ranges expected for neutron star accretors (Galloway 2000b). We suggest that Comptonisation continuum components are excellent candidates for fits to spectra from X-ray pulsars.

The sharp dip in the pulse profiles is clearly associated with an increase in the scattering optical depth  $\tau$  both for GX 1+4 (at distinctly different fluxes and phase-averaged

spectral conditions) and also for RX J0812.4–3114. It is true that the estimated significance is only convincing for the brightest observation of GX 1+4. We note however that the confidence interval limits for the pulse phase spectral fit parameters were determined by projecting the full  $p$ -dimensional confidence region (where  $p$  is the number of free parameters in the model) onto the axis corresponding to each parameter. This provides a conservative estimate of the confidence intervals for individual parameters (Lampton, Margon & Bowyer 1976) and so the true significance of the spectral variation may be much greater.

Variation in  $\tau$  with pulse phase is possible if the scattering region lacks rotational symmetry, e.g. is extended in one direction preferentially. In that case the maximum possible optical depth will be obtained when the line of sight to the observer coincides with the longest dimension of the scattering region. For the accretion column, the longest dimension is clearly along the column axis. Thus, we identify the sharp dips as ‘eclipses’ resulting from an approximate alignment of the accretion column with the line of sight, occurring once each rotation period ( $\phi = 0.0$  in Fig. 1). Absorption dips in the orbital lightcurves of some polars, which are white dwarf stars also accreting through a magnetically confined column (e.g. RX J1802.1+1804; Greiner, Remillard & Motch 1998), have previously been associated with a similar effect. The spectral variation in the latter source during the eclipse suggests a warm absorber, in good agreement with the results described here.

Clearly such interactions require a fortuitous combination of the magnetic colatitude  $\beta$  (the angle between the neutron star spin axis and the magnetic axis) and the inclination angle  $i$  (between the spin axis and the line of sight). Since the base of the accretion column is offset from the magnetic pole, and the column meets the surface at an angle with respect to the local normal,  $i$  must substantially greater than  $\beta$  for eclipses to occur. The column orientation also depends upon the inner disc radius  $r_{A,\text{disc}}$  since this defines which field lines connect the boundary region to the neutron star. The small number of sources exhibiting such eclipses (3 of more than 70 known pulsars) appears to be consistent with the relative unlikelihood of such an agreement; no reliable estimates of  $i$  and  $\beta$  have been made for the three pulsars described which might rule out this possibility.

While numerical simulations based on unmagnetized Compton scattering in a simplified emission region support this interpretation (Galloway & Wu 2001) it is important to note that the strong magnetic field present in the accretion column will significantly affect the scattering cross section (Daugherty & Harding 1986). The cross section  $\sigma(\nu, \theta)$  will depend on both the photon energy  $\nu$  and the angle between the propagation direction and the local magnetic field vector  $\theta$ . For GX 1+4, the estimated magnetic field strength implies an energy for the fundamental cyclotron resonance of  $h\nu_{\text{cyc}} \gtrsim 200$  keV, much greater than the PCA energy band. Thus for a particular photon energy,  $\sigma_{\nu, \theta}$  will reach a minimum for photons propagating along the magnetic field lines ( $\theta = 0$ ). In the absence of anisotropies in the distribution of matter this would result in enhanced emission along the magnetic axis. This effect will clearly compete with the decrease in emission due to the additional optical depth experienced by photons propagating along the accretion col-

umn. However  $\sigma_{\nu, \theta}$  reaches a minimum value (which depends upon the magnetic field strength and the photon energy) for photons propagating exactly along the magnetic field lines. The increase in optical depth is instead limited only by the geometry and the curvature of the accretion column. Despite magnetic anisotropy effects it should still be possible to get a significant drop in emission due to accretion column eclipses.

The observation of accretion column eclipses in GX 1+4 provides a unique opportunity to study accretion dynamics under the influence of a strong magnetic field. The variability in the observed phase of individual dips suggests that the column is wandering stochastically in longitude by  $2\text{--}6^\circ$ , depending upon the source luminosity. It is possible that the dip timing residuals are a consequence of variations in the  $P_{\text{spin}}$  itself, although we consider this unlikely. Accreting material typically possesses a large specific angular momentum with respect to the neutron star, and in combination with magnetic torques transmitted from the accretion disc via the magnetic field may induce systematic period evolution of more than 2 per cent per year. However the variations seen in the *RXTE* observations are typically of the same order in just one pulse period, and in addition there appears to be no cumulative drift in the pulse period on time-scales of tens of minutes or more as a consequence of the timing residuals. The accretion column is delineated by the ‘bundle’ of magnetic field lines which bound it, and it seems more likely that the position of the column is varying perhaps as a consequence of accretion along a varying set of field lines, resulting in a change in its apparent position.

The dip phase width  $w_d$  measured from both the mean pulse profiles and the average of the individual dip fits from each observation show a significant correlation with X-ray luminosity  $L_X$ . This parameter is a measure of the width of the accretion column, which ultimately depends upon the azimuthal extent of the accretion stream at the inner accretion disc boundary (see Fig. 1). The detailed physics of this boundary region are poorly understood, and so we assume that the entrainment of disc material to the column takes place at a rate which is independent of the plasma density in the disc. The column will then be wider at higher  $\dot{M}$  due to the increased velocity of disc plasma as the inner disc edge moves closer to the neutron star. The inner disc radius is determined by a balance of the magnetic stress and the ram pressure

$$\begin{aligned} r_{A,\text{disc}} &\approx 0.5 \times 2^{-3/7} \mu^{4/7} (GM_*)^{-1/7} \dot{M}^{-2/7} \\ &= 2.4 \times 10^8 B_{12}^{4/7} \dot{M}_{16}^{-2/7} \text{ cm} \end{aligned} \quad (1)$$

where  $\mu$  is the magnetic dipole moment,  $B_{12}$  is the corresponding surface magnetic field strength in units of  $10^{12}$  G,  $M_* = 1.5 M_\odot$ ,  $R_* = 10$  km the mass and radius of the neutron star and  $\dot{M} = \dot{M}_{16} \times 10^{16} \text{ g s}^{-1}$  the accretion rate (Ghosh & Lamb 1979a,b). Assuming that the plasma in the boundary region is still flowing tangentially at approximately the Keplerian velocity  $v_K = \sqrt{GM_*/r}$  corresponding to stable circular orbits, we have

$$w_d \propto \frac{v_K}{r_{A,\text{disc}}} \propto L_X^{3/7}. \quad (2)$$

The agreement between this relationship and the  $w_d$  measured from the individual dips is encouraging (Fig. 5b), al-

though the error bars on several points are large indicating significant variation of dip width for individual observations.

We note that the dip width measured for RX J0812.4–3114 on 1999 Mar 25 was  $w_d \approx 0.05$ , comparable to that measured in GX 1+4 at similar luminosity levels. If the conditions in the disc–magnetosphere boundary layer are similar in both pulsars, and relative bolometric corrections are negligible, this implies that the magnetic moments are similar and that the field strength for RX J0812.4–3114 is also around  $2\text{--}3 \times 10^{13}$  G. That these two pulsars, both with atypically strong magnetic fields, also possess an unusual alignment permitting accretion column eclipses seems rather unlikely however.

Since the dips are associated with interactions with the accretion column, they are expected to always be present so long as substantial amounts of material are accreting (i.e.  $\dot{M} \neq 0$ ). The *RXTE* observations of GX 1+4 span more than two orders of magnitude in  $L_X$ , and dips were observed in the mean pulse profiles of every observation except one. During a short *RXTE* observation on 1997 May 17, the dips were weak or absent in the lightcurve even though the phase-averaged countrate from the source was  $\approx 150$  counts  $s^{-1}$ , still well above the background which is typically 100 counts  $s^{-1}$ . The X-ray spectrum measured at this time was unusually hard, with Compton scattering optical depth  $\tau \approx 19$ ; the pulse-phase spectral variation was also substantially different from that measured at other times (Galloway 2000a). Both the disappearance of the dip and the spectral measurements indicate a distinctly different accretion regime than is normal for this source, in which the column is no longer present in the usual sense.

This work has revealed some important new phenomena likely to be common to other X-ray pulsars. Further observational and theoretical development appears promising, in particular where the unusual properties of sources like GX 1+4 and RX J0812.4–3114 may be exploited. The influence of the longitudinal variation in column position on the net torque transmitted to the neutron star may be non-negligible. This may affect the long-term period evolution in persistent pulsars, which is generally rather poorly understood (e.g. Bildsten et al. 1997). Measurements of the dip (and hence column) profile may provide more detailed information regarding the plasma uptake to the accretion column at the inner disc radius. Finally, the suggestion of disruption of the accretion column coupled with distinct spectral states at high and low luminosities (Galloway 2000b) provides evidence for significantly more complex flow dynamics than are predicted by current theory.

## ACKNOWLEDGMENTS

This research has made use of data obtained from the BATSE pulsar group home page at <http://www.batse.msfc.nasa.gov>, and also the High Energy Astrophysics Science Archive Research Center Online Service, provided by the NASA/Goddard Space Flight Center. The *RXTE* Guest Observer Facility provided timely and vital help and information throughout.

## REFERENCES

- Belczyński K., Mikołajewska J., Munari U., Ivison R. J., Friedjung M., 2000, *A&AS*, 146, 407
- Beurle K., Bewick A., Harper P., Quenby J., Spooner N., Fenton A., Fenton K., Giles A., et al., 1984, *AdSpR*, 3(10–12), 43
- Bildsten L., Chakrabarty D., Chiu J., Finger M. H., Koh D. T., Nelson R. W., Prince T. A., Rubin B. C., et al., 1997, *ApJS*, 113, 367
- Čemeljić M., Bulik T., 1998, *Acta Astronomica*, 48, 65
- Chakrabarty D., Bildsten L., Finger M. H., Grunsfeld J. M., Koh D. T., Nelson R. W., Prince T. A., Vaughan B. A., et al., 1997, *ApJL*, 481, L101
- Chakrabarty D., Roche P., 1997, *ApJ*, 489, 254
- Corbet R. H. D., 1986, *MNRAS*, 220, 1047
- Corbet R. H. D., Peele A. G., 2000, *ApJL*, 530, L33
- Cui W., 1997, *ApJL*, 482, L163
- Daugherty J. K., Harding A. K., 1986, *ApJ*, 309, 362
- Davidson A., Malina R., Bowyer S., 1977, *ApJ*, 211, 866
- Dotani T., Kii T., Nagase F., Makishima K., Ohashi T., Sakao T., Koyama K., Tuohy I. R., 1989, *PASJ*, 41, 427
- Galloway D. K., 2000a, *ApJL*, 543, L137
- , 2000b, *ApJ*, submitted (astro-ph/0007274)
- Galloway D. K., Giles A. B., Greenhill J. G., Storey M. C., 2000, *MNRAS*, 311, 755
- Galloway D. K., Wu K., 2001, in *X-ray Astronomy '999 — Stellar Endpoints, AGN and the Diffuse Background*. Bologna, Malaguti G., Palumbo G., White N., eds., Gordon & Breach, Singapore
- Ghosh P., Lamb F. K., 1979a, *ApJ*, 232, 259
- , 1979b, *ApJ*, 234, 296
- Giles A. B., Galloway D. K., Greenhill J. G., Storey M. C., Wilson C. A., 2000, *ApJ*, 529, 447
- Greenhill J. G., Sharma D. P., Dieters S. W. B., Sood R. K., Waldron L., Storey M. C., 1993, *MNRAS*, 260, 21
- Greiner J., Remillard R. A., Motch C., 1998, *A&A*, 336, 191
- Jahoda K., Swank J. H., Giles A. B., Stark M. J., Strohmayer T., Zhang W., Morgan E. H., 1996, *Proc. SPIE*, 2808, 59
- Lampton M., Margon B., Bowyer S., 1976, *ApJ*, 208, 177
- Mony B., Kendziorra E., Maisack M., Staubert R., Englhauser J., Dobreiner S., Pietsch W., Reppin C., et al., 1991, *A&A*, 247, 405
- Motch C., Haberl F., Dennerl K., Pakull M., Janot-Pacheco E., 1997, *A&A*, 323, 853
- Negueruela I., Reig P., Finger M., Roche P., 2000, *A&A*, 356, 1003
- Pereira M. G., Braga J., Jablonski F., 1999, *ApJL*, 526, L105
- Press W. H., Teukolsky S. A., Vetterling W. T., Flannery B. P., 1996, *Numerical Recipes in Fortran 77: The Art of Scientific Computing*, 2nd edn. Cambridge University Press, Cambridge, New York, Melbourne
- Reig P., Roche P., 1999, *MNRAS*, 306, 95
- Titarchuk L., 1994, *ApJ*, 434, 570
- Warner B., 1995, *Cataclysmic Variable Stars*, 1st edn. Cambridge University Press, Cambridge, pp. 1–572
- White N. E., Nagase F., Parmar A. N., 1995, in *X-ray Binaries*, Lewin W. H. G., van Paradijs J., van den Heuvel E. P. J., eds., Cambridge University Press, Cambridge, pp. 1–57
- Zhang S. N., Harmon B. A., Fishman G. J., Paciasas W. S., 1995, *Experimental Astronomy*, 6, 57

This paper has been produced using the Royal Astronomical Society/Blackwell Science  $\LaTeX$  style file.